NUMERICAL INVESTIGATION OF THE HEAT-TRANSFER PROBLEM SIMULATING THE ZONE MELTING PROCESS

B. M. Anisyutin

UDC 517.9

The floating zone method is the most widespread crucible-free method of purifying materials and growing monocrystals. The mechanics of the material purification process is that melting of a certain interior section of the vertical cylindrical ingot rod is performed in the initial stage, while the melted zone is displaced slowly along the rod in the second stage. The monocrystal growing process is similar to the purification process except that in the initial stage a tip rather than an interior section of the purified rod is melting, and is then set in contact with the monocrystalline "seed" of this substance. Three aspects of this problem can be extracted conditionally for a theoretical study: the melt stability, the hydrodynamic phenomena in the floating zone, and the heat transfer in the system in the absence of convection in the melt. When investigating the first two directions the authors ordinarily assume that the temperature distribution and the location of the melt boundary are known a priori [1-3]. Therefore, the geometric characteristics of the melted zone and the temperature distribution in the specimen must be known for a correct formulation of the hydrodynamic problems and the stability problem.

Sufficiently many diverse methods are used at this time to solve the Stefan problem that occurs. But the specifics of zone melting is that the displacement of the melted zone is extremely slow (on the order of 1 cm/h) and it can be neglected. In this case the volume of the calculations is successfully reduced substantially since the problem with a free boundary goes over into a boundary-value problem for the Laplace equation in a known domain after the Kirchhoff transformation. Such an approach to the solution of the stationary Stefan problem was first applied in [4], where the temperature distribution and the shape of the phase transition front were determined numerically under the following assumptions: 1) the system is in the steady state, the melt boundaries are fixed, the temperature depends only on two variables (the radius and longitudinal coordinate); 2) there is no convection in the melt; 3) the rod is in a vacuum; 4) the physical properties of each phase are independent of the temperature; 5) the free surface of the liquid phase is cylindrical; 6) both rod tips are heat-insulated.

In this paper the axisymmetric stationary problem of finding the temperature distribution and the location of the phase interface is investigated numerically under assumptions 1-4. As compared with [4], the additional difficulty is associated with the fact that the lateral surface of the liquid phase is considered free and depends on capillary forces [2].

A new boundary condition simulating the attachment of the specimen to the heat-conducting rod is given at the ingot endfaces. In particular, it permits reduction in the volume of the calculations if fictitious boundaries are introduced and an internal shorter ingot section attached to rods of the same material is considered.

The following results are obtained: the critical powers of the external heat sources are obtained, at which the melt domain is formed, a liquid bridge occurs, the phase transition fronts became practically planar; the structure of the phase interfaces is studied as a function of the power and the method of focusing the heat source. The strong dependence of the phase interfaces on the problem parameters is exposed in the case of small melted zone sizes.

1. Formulation of the Problem. An axisymmetric specimen $\omega = \{(r, z) | 0 < r < g(z), d_1 < z$ of length $\ell = d_2 - d_1$ is considered in which has phases are present: liquid ω^+, where the temperature T is above the melting point T_*, and the solid ω^-, where $T < T_*$. It is assumed that T(r, z) depends only on two variables, the radius r and the coordinate z directed

Novokuznetsk. Translated from Zhurnal Prikladnoi Mekhaniki i Tekhnicheskoi Fiziki, No. 2, pp. 71-77, March-April, 1988. Original article submitted December 29, 1986.

0021-8944/88/2902-0225$12.50

TABLE 1

Sketch number	H	N	C	D_1	D_2	P	D_5	$\pi-\beta$
1	0,01	0	1	—20	20	0,108—0,180	2,0	0
2	0,01	0	1	—20	20	0,08—0,18	0,5	0
3	1	0	1	—20	20	4,2—14,0	2,0	0
4	1	0	1	—20	20	2,0—14,0	0,5	0
5	0,01	0—2	1	—35	5	0,12	2,0	0
6	0,01	0	1	—20	20	0—0,24	0,5—2,0	0
7	1	0	1	—20	20	0—15	0,5—2,0	0
8	0,01	1	1	—20	20	0,11	0,5—2,0	0
9	0,01	0	0,5—2	—20	20	0,11	2,0	0
10	0,01	0	1	—20	20	0,11	2,0	—0,2—0,2

along the axis of symmetry and satisfies the Laplace equation

$$\Delta T = 0 \text{ in } \omega^{\pm}. \tag{1.1}$$

in each phase. On the specimen endfaces we set

$$\varkappa \partial T/\partial n = -\mu T^{5/2} \text{ as } \quad z = d_i, \ i = 1, 2. \tag{1.2}$$

Condition (1.2) resulted from the following reasoning. In experiments, say, a silicon specimen is fastened to a copper rod. Since copper is a good heat conductor, the temperature distribution in the copper rod can be considered uniform and satisfying the problem [5]

$$R_0 \tilde{\varkappa} \tilde{T}_{zz} = 2\tilde{\varepsilon}\sigma \tilde{T}^4, \ z > d_2, \quad \tilde{T}_z = 0, \ z = +\infty, \ \tilde{T} = T_2, \ z = d_2, \tag{1.3}$$

which has the exact solution

$$\tilde{T} = T_2 \left(1 + \sqrt{\frac{1.8\tilde{\varepsilon}\sigma}{\tilde{\varkappa} R_0}} T_2^3 (z - d_2)\right)^{-2/3}, \ z > d_2. \tag{1.4}$$

Since the temperature and heat flux are continuous on the material interface from physical considerations: $T = \tilde{T} = T_2$, $\varkappa \partial T/\partial n = \tilde{\varkappa}\, \partial \tilde{T}/\partial n$, $z = d_2$, then for z = d_2 we have (1.2) with $\mu = \sqrt{0.8\tilde{\varepsilon}\tilde{\varkappa}\sigma/R_0}$. Condition (1.2) is obtained analogously for z = d_1.

The radiation condition in a vacuum according to the Stefan–Boltzmann law

$$\varkappa \partial T/\partial n = -\varepsilon(\sigma T^4 - q(z)) \text{ for } \quad r = g(z), \tag{1.5}$$

is satisfied on the lateral surface, where κ, ϵ, σ are the heat conduction, emissivity, and Boltzmann coefficients, respectively, q(z) is the external heat flux, aud n is the unit external normal to the lateral surface.

On the axis of symmetry we set

$$T_r = 0 \text{ for } \quad r = 0. \tag{1.6}$$

The temperature on the phase interface equals the melting point

$$T = T_* \text{ on } \gamma \tag{1.7}$$

and the Stefan condition is satisfied, which takes the form of equality of the heat fluxes in the stationary case

$$\varkappa_l \partial T_l/\partial n_1 = \varkappa_s \partial T_s/\partial n_1 \text{ on } \gamma \tag{1.8}$$

(n_1 is the unit normal to the phase transition surface).

The heat-conduction coefficient is assumed a piecewise-constant function of the temperature

$$\varkappa(T) = \begin{cases} \varkappa_s, & T < T_*, \\ \varkappa_l, & T > T_*. \end{cases}$$

2. Reduction to a Problem for the Laplace Equation. Let us perform the Kirchhoff transformation

$$U(T) = \frac{1}{\varkappa_s T_*} \int_{T_*}^{T} \varkappa(s)\, ds = \frac{T - T_*}{c(T)\, T_*}, \tag{2.1}$$

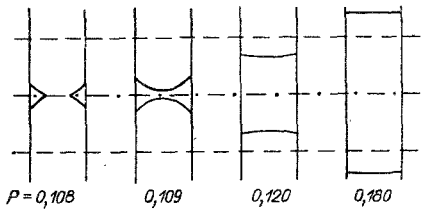

Fig. 1

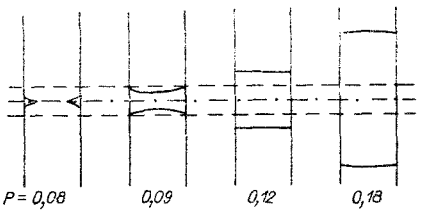

Fig. 2

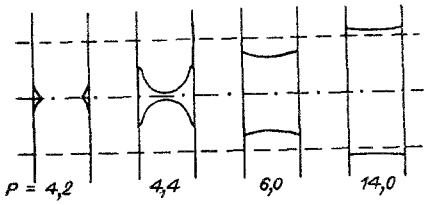

Fig. 3

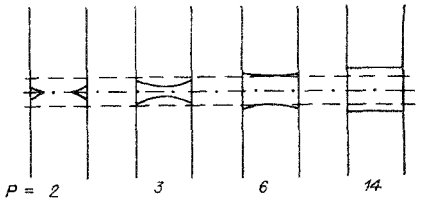

Fig. 4

where c(T) = 1 for $T < T_*$ and $c(T) = C \equiv \kappa_s/\kappa_l$ for $T > T_*$ and the substitution

$$x = r/g(z),\ y = z/R_0 \tag{2.2}$$

($R_0 = g(d_1)$ is the radius of the ingot). The curvilinear domain ω here goes over into the rectangle $\Omega = (0, 1) \times (D_1, D_2)$. The dimensionless reduced temperature U(x, y) satisfies an elliptical equation in the domain Ω

$$a_{11}U_{xx} + a_{12}U_{xy} + U_{yy} + a_1U_x = 0 \text{ в } \Omega, \tag{2.3}$$

on the boundaries

$$U_y = \nu(cU + 1)^{5/2} \text{ for } y = D_1; \tag{2.4}$$

$$U_y = -\nu(cU + 1)^{5/2} \text{ for } y = D_2; \tag{2.5}$$

$$b_1U_x + b_2U_y = -H(cU + 1)^4 + Q \text{ for } x = 1; \tag{2.6}$$

$$U_x = 0 \text{ for } x = 0; \tag{2.7}$$

$$a_{11} = \frac{1}{G^2} + \left(x\frac{G'}{G}\right)^2,\ a_{12} = -2x\frac{G'}{G}, \tag{2.8}$$

$$a_1 = \frac{1}{xG^2} + x\frac{2(G')^2 - GG''}{G^2},\ b_1 = \frac{\sqrt{1 + (G')^2}}{G},\ b_2 = -\frac{G'}{\sqrt{1 + (G')^2}}.$$

Four dimensionless parameters

$$H = \varepsilon\sigma R_0T_*^3/\kappa_s \text{ — Biot number},$$
$$\nu = \mu\frac{R_0}{\kappa_s}T_*^{3/2} = \sqrt{\frac{\widetilde{\varkappa\varepsilon}}{\varkappa\varepsilon}}\sqrt{0.8H} \equiv N\sqrt{0.8H},\ C = \kappa_s/\kappa_l,\ L = l/R_0, \tag{2.9}$$

and two functions

$$G(y) = g(R_0y)/R_0 \text{ (gives the lateral surface)},\ Q(y) = \frac{\varepsilon R_0q(R_0y)}{\kappa_sT_*} \text{ (defines the external heat flux)}. \tag{2.10}$$

are in the problem (2.3)-(2.7).

The solution U of the elliptical equation with smooth coefficients has continuous first derivatives everywhere within the domain Ω, consequently, the Stefan condition (1.8), which is equivalent to the continuity of the first derivatives of the function U in $\Gamma \subset \Omega$, is satisfied automatically. The equality of the temperature on the phase transition boundary to the melting point (1.7) permits finding the boundary Γ as the zeroth level line of the function U(x, y).

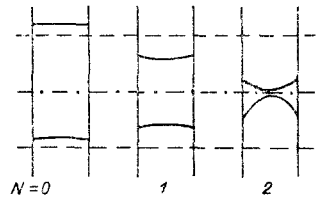

Fig. 5

3. Determination of the Lateral Surface. The shape of the free lateral melt surface G(y) in parametric form is found from the condition of capillary equilibrium in terms of the boundary angle β and the boundary of the melted zones D_3, D_4 as follows [2]: G(y) = 1 for $y \in [D_1, D_3] \cup [D_4, D_2]$, and for $y \in (D_3, D_4)$ as the solution of the system

$$y(\theta, \lambda) = D_3 + \int_{\lambda}^{\theta} \frac{1 + b\cos\xi}{f(\lambda, \lambda) f(\xi, \lambda)}\, d\xi,$$

$$D_4 = y(2\pi - \lambda, \lambda),\ G(\theta, \lambda) = f(\theta, \lambda)/f(\lambda, \lambda)$$

for $\lambda \le \theta \le 2\pi - \lambda$, when $f(\theta, \lambda) = \sqrt{1 + b^2 + 2b\cos\theta}$; $b = -\mathrm{tg}\,\beta\,/(\sin\lambda + \mathrm{tg}\,\beta\cos\lambda)$.

4. Numerical Solution of the Problem (2.3)-(2.7). The build-up method is used for the numerical solution, namely: an auxiliary problem is considered for an equation of parabolic type

$$v_t = a_{11}v_{xx} + a_{12}v_{xy} + v_{yy} + a_1 v_x \text{ in } \Omega\times(0,\ \infty); \tag{4.1}$$

$$v_t = v_y - \nu(cv + 1)^{5/2} \text{ for } y = D_1; \tag{4.2}$$

$$v_t = -v_y - \nu(cv + 1)^{5/2} \text{ for } y = D_2; \tag{4.3}$$

$$v_t = -b_1 v_x - b_2 v_y - H(cv + 1)^4 + Q \text{ for } x = 1; \tag{4.4}$$

$$v_x = 0 \text{ for } x = 0; \tag{4.5}$$

$$v = 0 \text{ for } t = 0. \tag{4.6}$$

Here $a_{11}, a_{12}, a_1, b_1, b_2, H, \nu, c, Q$ are determined from (2.8)-(2.10). If $\lim \nu_t = 0$ as $t \to \infty$, then

$$U_*(x, y) = \lim_{t\to\infty} v(x, y, t) \tag{4.7}$$

is a solution of the problem (2.3)-(2.7).

A locally one-dimensional second-order difference scheme of approximation in the spatial variables is used to solve the problem (4.1)-(4.6) [6, p. 413]:

$$(\bar{v} - v^{(n)})/\tau = \bar{v}_{\bar{y}y} + f \text{ in } \Omega; \tag{4.8}$$

$$(v^{(n+1)} - \bar{v})/\tau = a_{11}v^{(n+1)}_{\bar{x}x} + f \text{ in } \Omega\ \left(f = (1/2)\left(a_{12}v^{(n)}_{\dot{x}\dot{y}} + a_1 v^{(n)}_{\dot{x}}\right)\right). \tag{4.9}$$

The boundary conditions are also second-order approximations

$$(\bar{v} - v^{(n)})/\tau = v^{(n)}_{\hat{y}} - \nu\left(cv^{(n)} + 1\right)^{5/2} \text{ for } y = D_1; \tag{4.10}$$

$$(\bar{v} - v^{(n)})/\tau = -v^{(n)}_{\hat{y}} - \nu\left(cv^{(n)} + 1\right)^{5/2} \text{ for } y = D_2; \tag{4.11}$$

$$(v^{(n+1)} - v^{(n)})/\tau = -b_1 v^{(n)}_{\hat{x}} - b_2 v^{(n)}_{\dot{y}} - H\left(cv^{(n)} + 1\right)^4 + Q \text{ for } x = 1; \tag{4.12}$$

$$v^{(n+1)}_{\hat{x}} = 0 \text{ for } x = 0; \tag{4.13}$$

$$v = 0 \text{ for } t = 0. \tag{4.14}$$

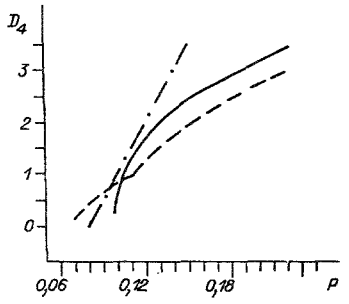

Fig. 6

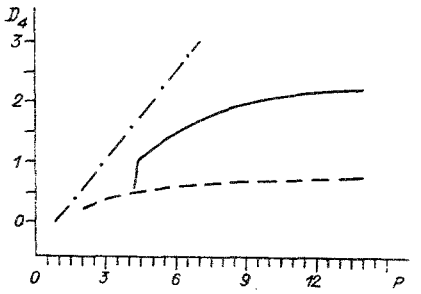

Fig. 7

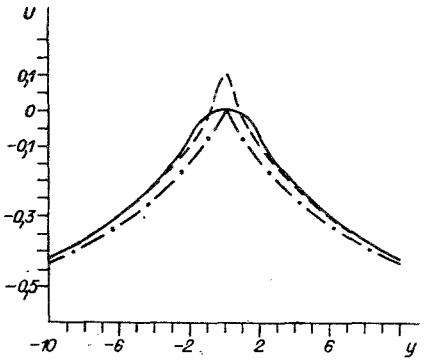

Fig. 8

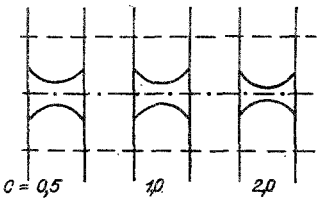

Fig. 9

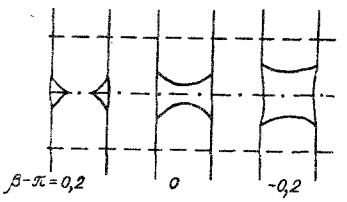

Fig. 10

Remark 1. Introduction of the time derivative v_t in the nonlinear boundary conditions (4.2)-(4.4) permitted us to obtain the second-order approximations in the spatial variables easily in their difference analog (4.10)-(4.12).

5. Description of Program Operation. 1) The constants D_i, $i = 1, \ldots, 5$, C, H, ν, β, P are given; 2) the lateral surface G(y) is determined by means of β, D_3, D_4; 3) the coefficients of the equation are found; 4) the external heat flux Q(y) is selected such that

$$Q(y)\,G(y) = \begin{cases} Q_*, & |y| < D_5, \\ 0, & |y| > D_5; \end{cases} \tag{5.1}$$

then the power is calculated from the formula

$$P = 2Q_*D_5, \tag{5.2}$$

the relationships (5.1) and (5.2) define the function Q(y) as a function of P and D_5; 5) the problem (4.8)-(4.14) is solved by build-up: $U = v^{(n)}$ if $\max\limits_{ij} |v^{(n)} - v^{(n-1)}| < 10^{-5}$; 6) on the basis of linear interpolation the level lines of U(x, y) = 0 are found that agree with the phase interfaces.

Remark 2. To determine the lateral surface G(y) by means of the formulas described in Sec. 3, three parameters must be known: β, D_3, D_4. The boundary angle β is considered known for this process while the points D_3 and D_4 are the boundaries of the melted zone by the physical meaning, i.e., not only the reduced temperature U but also the points D_3 and D_4 are desired in the problem (2.3)-(2.7). Consequently, additional calculations are needed that are constructed in such a manner: firstly we set $D_4^{(0)} = -D_3^{(0)} = R_0$, satisfying steps 2-6, the first approximation of the phase interface $D_i^{(1)}$ is found; continuing this process the sequence $D_i^{(k)}$ is obtained. If $\max\limits_{i=3,4} |D_i^{(k)} - D_i^{(k-1)}| < 0.01$, then it is considered that $U^{(k)}$, $D_3^{(k)}$, $D_4^{(k)}$ is a solution of problem (2.3)-(2.7).

6. Results of a Computation. Displayed in Figs. 1-5 and 9-10 are sections of the radial rod section $|z| < 3.5R_0$ on which the dash-dot line corresponds to z = 0, the dashes to $|z| = D_5$ and the solid line to the phase interface Γ. The set of values of parameters for Figs. 1-10 are given in the table.

Presented in Figs. 1-4 are the characteristic profiles of the phase interfaces in the case of heat-insulated tips as a function of the heat source power. These results are in good agreement with the computations [4].

Shown in Fig. 5 is the influence of the heat flux through the ingot endfaces on the melt geometry as the floating zone moves to one of the ends; N = 1 simulates the case when the final short section is considered in an infinitely long ingot. As should have been expected, the melted zone here has a symmetric shape while the temperature distribution in the solid phased differs slightly (by less than 0.01) from that obtained from the one-dimensional model [5]

$$U_D(y) = \begin{cases} [1 + \sqrt{1.8H}\,(y - D_4)]^{-2/3} - 1, & y \geqslant D_4, \\ 0, & D_3 < y < D_4, \\ [1 - \sqrt{1.8H}\,(y - D_3)]^{-2/3} - 1, & y \leqslant D_3. \end{cases} \tag{6.1}$$

Represented in Figs. 6 and 7 is the dependence of the melted zone halfwidth on the lateral surface D_4 on the heat source power P for different Biot numbers. The dashed line corresponds to narrow heat flux ($D_5 = 0.5$), the solid line to a broader ($D_5 = 2$), and the dash–dot to the dependence

$$P = \sqrt{0.8H} + 2HD_4, \tag{6.2}$$

obtained from the one-dimensional model [5].

Shown in Fig. 8 is the distribution of the reduced temperature U on the specimen surface x = 1 (the solid line is $D_5 = 2$, the dashes to $D_5 = 0.5$, and the dash–dots to the temperature distribution (6.1) from the one-dimensional model [5] for $D_3 = D_4 = 0$).

It is seen from Figs. 6-8 that for small Biot numbers the dependence (6.2) permits a sufficiently good estimation of the power needed to form the floating zone, and the temperature distribution from (6.1). Let us note that for small melted zones, small fluctuations in the power P result in significant changes in D_4, as follows from Figs. 6 and 7. In this case the phase interface depends strongly on other parameters of the problem also, for instance, the relationships between the heat-conduction coefficients of the liquid and solid phases C (Fig. 9), or the shapes of the free melt surfaces (Fig. 10). Such a dependence of the melt size on the problem data is explained by the fact that variation of the parameters of the problem result in small temperature fluctuations, and since the temperature gradient near the phase transition boundary is small (Fig. 8), then the shift of the isoline U = 0 or, equivalently, the displacement of the phase interface turns out to be perceptible.

Associated with this are difficulties, in principle, in the numerical determination of the melt boundaries since the process converges slowly and large expenditures of machine time are required. The results presented in Figs. 1-10 are obtained on the electronic computers ES 1052, 1061 on a 11 × 41 point mesh for $\tau = 0.1$. The computations carried out on finer meshes showed that the qualitative properties of the solutions are reflected truly.

In conclusion, we note the following: 1) if the melted zone is sufficiently far from the ingot endfaces, then by considering considerably shorter sections of the rod with the boundary conditions (2.4) and (2.5) for $\nu = \sqrt{0.8H}$, a good approximation can be obtained for the temperature distribution on this section; 2) for small values of the melted zone width the melt geometry depends strongly on the parameters of the problem; 3) for large values of D_5 the process can be in the domain of a strong dependence of the melt geometry on the problem parameters even for a melted zone length of $D_4 - D_3 \approx 2\pi$ on the ingot surface.

The author is grateful to V. V. Pukhnachev and L. G. Badratinova for formulating the problem and discussing the results.

LITERATURE CITED

1. L. A. Slobozhanin, "Investigation of the hydrostatic problems simulating the zone melting process," Third All-Union Seminar on Hydromechanics and Heat and Mass Transfer in Weightlessness." Abstracts of Reports [in Russian], Chernogolovka (1984).
2. L. G. Badratinova, "Stability of axisymmetric equilibrium modes of a capillary fluid in a cylindrical ampoule," Dynamics of a Continuous Medium [in Russian], Inst. Hydrodyn. Sib. Branch USSR Acad. Sci., No. 63 (1983).

3. E. D. Lyumkis, B. Ya. Martuzan, and E. N. Martuzane, "Interaction of fluxes caused by thermocapillary convection and rotation during zone melting and their influence on the propagation of impurities," Technological Experiments in Weightlessness [in Russian], Sverdlovsk (1983).
4. N. Kobayashi, "Power required to form a floating zone and zone shape," J. Crystal Growth, 43, 417 (1978).
5. D. K. Donald, "Thermal mode under vacuum melting conditions," Rev. Sci. Instrum., No. 7 (1961).
6. A. A. Samarskii, Introduction into the Theory of Difference Schemes [in Russian], Nauka, Moscow (1971).

STEADY-STATE CONFIGURATIONS OF THE DEFORMATION REGION AND THE FORCE BALANCE IN THE DRAWING OF AN OPTICAL FIBER

V. N. Vasil'ev and V. D. Naumchik

UDC 532.522 + 681.7.068.4

Fiber light guides are thin glass fibers formed from a liquid mass drawn through a die or pulled from a cylindrical semifinished product as a result of its symmetrical local heating to about 2000°C. Passing through air, the quartz glass melt forms a liquid stream with a free surface whose form is determined by the equilibrium between the forces of internal friction, surface tension, gravity, friction against the air, the force of acceleration on the glass, and the shearing force. The stream cools as it descends and, after application of the first polymer coating, the cold fiber enters a rotating drum. The drum maintains tension in the stream, forcing it to become thinner as cooling proceeds. The behavior of the molten stream of quartz glass can be examined on the basis of the gasdynamic equations of an incompressible Newtonian fluid and the energy equations, since the equation of motion contains the absolute viscosity – which is a function of temperature. Recent experimental findings show that shear flow occurs during the drawing of optical fibers [1]. Until now, there has been no reliable theory for calculation of the two-dimensional distribution of temperature and velocity in a jet of a high-viscosity liquid with a free surface. Thus, it is usually the practice to make several assumptions (examined in more detail in [2]) which make it possible to reduce the problem to a unidimensional problem. However, no detailed analysis of the drawing of optical fibers has been made even within the framework of unidimensional models. Here, the approaches have been either to solve only the hydrodynamic problem and assume that the viscosity distribution along the deformation is simply prescribed or to introduce an excessively simplified energy equation which does not adequately describe the process of heat transfer during fiber drawing.

Here, we examine the main results of a study of the formation of optical fibers obtained on the basis of a quasiunidimensional mathematical model whose basis principles were described in [3]. We will also analyze the balance of the forces acting in the deformation region during the formation of a fiber by the bead method.

1. The process of the formation of an optical fiber is examined in the simple uniaxial tension of a Newtonian fluid with variable viscosity determined by the temperature distribution. The temperature distribution is found from the energy equation. In formulating the system of equations describing the dynamics of fiber drawing, it was assumed that except for viscosity, the physical properties of the liquid are constant, the liquid is isotropic, and its motion is axisymmetric.

The equations of continuity

$$-\frac{\partial R}{\partial \tau} = v\frac{\partial R}{\partial x} + \frac{R}{2}\frac{\partial v}{\partial x}; \qquad (1.1)$$

Leningrad. Translated from Zhurnal Prikladnoi Mekhaniki i Tekhnicheskoi Fiziki, No. 2, pp. 77-84, March-April, 1988. Original article submitted January 4, 1987.

0021-8944/88/2902-0231$12.50